ACS OMEGA

http://pubs.acs.org/journal/acsodf

Article

Exfoliated Graphite Nanoplatelet-Carbon Nanotube Hybrid Composites for Compression Sensing

Changyoon Jeong and Young-Bin Park*

Cite This: *ACS Omega* 2020, 5, 2630−2639

Read Online

ACCESS | Metrics & More | Article Recommendations

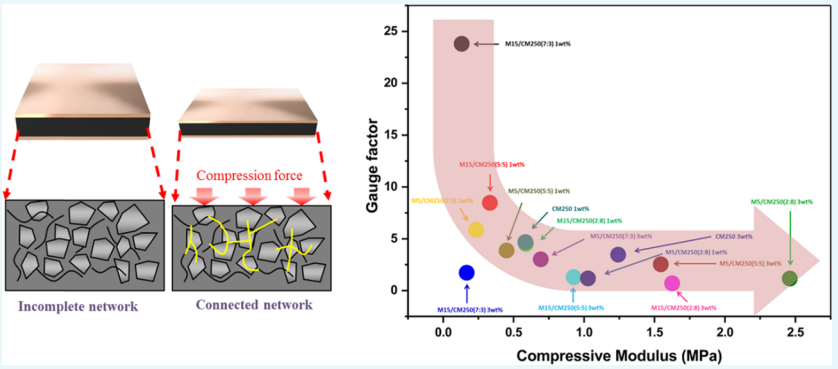

ABSTRACT: In this study, we investigated the gauge factor and compressive modulus of hybrid nanocomposites of exfoliated graphite nanoplatelets (xGnP) and multiwalled carbon nanotubes (MWCNTs) in a polydimethylsiloxane matrix under compressive strain. Mechanical and electrical tests were conducted to investigate the effects of nanofiller wt %, the xGnP size, and xGnP:MWCNT ratio on the compressive modulus and sensitivity of the sensors. It was found that nanofiller wt %, the xGnP size, and xGnP:MWCNT ratio significantly affect the electromechanical properties of the sensor. The compressive modulus increased with an increase in the nanofiller wt % and a decrease in the xGnP size and xGnP:MWCNT ratio. However, the gauge factor decreases with a decrease in the nanofiller wt % and xGnP size and an increase in the xGnP:MWCNT ratio. Therefore, by investigating the piezoresistive effects of various factors for sensing performance, such as wt %, xGnP size, and xGnP:MWCNT ratio, the concept of one- and two-dimensional hybrid fillers provides an effective way to tune both mechanical properties and sensitivity of nanocomposites by tailoring the network structure of fillers.

INTRODUCTION

Carbon nanomaterials such as carbon nanotubes (CNTs), carbon black (CB), graphite, and graphene exhibit outstanding electrical properties and can easily form electrically conductive networks in various nonconductive polymer materials under the application of an external force.[1−18] These unique properties of carbon nanomaterials have been utilized for the development of sensitive strain sensors responding to external forces (compression, tension, etc.). For realizing the practical applications of carbon nanomaterials for the development of sensing devices, carbon nanocomposites consisting of a matrix and carbon nanofillers have been used. Especially, various efforts have also been made to functionalize carbon nanofillers for enhancing their electromechanical properties. The carbon fillers such as CNTs,[2,19,20] functionalized CNTs,[21,22] CB,[8,10,23,24] graphite,[11,25−27] and graphene[28−32] have been used to fabricate nanocomposites for sensing devices. The dispersion of nanofillers in the matrix and their properties and sensing capabilities can be optimized by controlling the processing conditions, raw material properties, nanofiller weight fraction (wt %), nanofiller conductivity, and barrier height of the polymer matrix.[33−37] The electrical properties of these carbon nanomaterials in nonconductive polymers have been investigated and verified by the tunneling effect to characterize the sensing capability of randomly distributed carbon nanoparticles in polymer matrices.[38−43] However, in all the previous studies carried out in this context, a single carbon nanomaterial was used in the polymer matrix. Recently, hybrid nanocomposites consisting of two types of carbon nanomaterials have been reported.[4,11,44,45] These hybrid nanocomposites showed better mechanical properties, optical energy densities, and piezoresistivities than nanocomposites consisting of a single carbon nanomaterial in the polymer. However, the material properties of these nanocomposites

Received: September 15, 2019
Accepted: January 24, 2020
Published: February 3, 2020

https://dx.doi.org/10.1021/acsomega.9b03012
ACS Omega 2020, 5, 2630−2639

limit their practical applications due to their flexibility and sensitivity under compression. Sensing performance and mechanical properties of the hybrid nanocomposites consisting of carbon black and CNTs have been investigated, but there has been rather limited research on the electromechanical properties of flexible nanocomposites consisting of one-dimensional (1D) and two-dimensional (2D) fillers under compressive loading.[46−49] It would be of great research interest to investigate the physical interactions between the 1D and 2D nanofillers and how they affect the conductive path formation and piezoresistivity. It is also important to understand the correlation between the geometries, for example, length and lateral dimensions, of 1D and 2D conductive nanofillers and the electromechanical properties of hybrid nanocomposites. In this study, we fabricated a compressive strain sensor using a hybrid nanocomposite consisting of 1D multiwalled CNTs (MWCNTs) and 2D exfoliated graphite nanoplatelets (xGnPs) in a polydimethylsiloxane (PDMS) matrix. The MWCNTs and xGnPs interacted easily with each other under compression. We also investigated the piezoresistive effect of the composite sensor and the synergistic effect of the MWCNTs and xGnPs on the electrical and mechanical properties of the hybrid nanocomposites. We used xGnPs with different diameters (M5 or M15) and MWCNTs (CM250) at various concentrations (wt %) for the preparation of the hybrid nanocomposites. The relationship between the electrical properties and mechanical compressive strain of the sensors was also investigated. Therefore, this study will be helpful for developing hybrid nanocomposite compression sensors.

RESULTS AND DISCUSSION

We fabricated flexible piezoresistive compression sensors with nanofiller wt %, two types of xGnPs with a difference in size, and various xGnP:MWCNT ratios (Table 1). Fabricated samples are easily deformed in compression for their flexibility and show piezoresistive effect. The electrical properties of nanocomposites were optimized by controlling the dispersion and distribution of carbon nanofillers in the matrix (Scheme 1). For dispersing carbon nanofillers in the polymer matrix, carbon nanofillers and PDMS are poured into a paste cup, and the resulting mixture was homogeneously dispersed using a paste mixer (500 revolutions and 400 rotations). After stirring it for 30 min, the mixture was further dispersed using the three-roll mill process with intense mechanical stirring. This mechanical stirring process was repeated more than 10 times. The well-dispersed mixture was then transferred to a mold. Mixtures consisting of carbon nanofillers in the polymer matrix were solidified at a high temperature (120 °C) and pressure (0.5 MPa) to finally obtain the hybrid nanocomposites with smooth surfaces and evenly dispersed carbon nanomaterials in the polymer matrix. The composites had a width, length, and height of 20, 20, and 1 mm, respectively. Finally, two Cu sheet electrodes were pasted at the top and bottom of the nanocomposites, and a mechanical force was applied to measure the *z*-axis resistance variations of the composites.

To investigate the behaviors of the carbon nanomaterials (xGnPs and MWCNTs) in the polymer matrix under compression, we characterized the composite for investigating material interaction under compression by using Raman spectroscopy. Hybrid nanocomposites were placed between two cover glasses to measure the characteristic band changes of carbonaceous materials under compression as shown in Figure 1a. The sample surfaces were irradiated with a laser operating at 532 nm. To apply compressive stresses on the nanocomposites, two equal weights were placed on the cover glass symmetrically. The weights were increased in 200 g steps from 0 to 400 g, and Raman spectra were obtained in each step. Raman spectra exhibiting the G, D, and 2D peaks of pristine CNTs and xGnPs and the C−H peak of PDMS are shown in Figure 1b. The 2D peaks for the hybrid nanocomposites were recorded after each weight increasing step. As compressive loads are applied to a nanocomposite (xGnP:MWCNT ratio of 5:5 was chosen as an example), Raman spectra shows 2D peak shifts as evidenced in Figure 1c, which indicates load transfer from the polymer matrix to carbon nanomaterials.[50,51] As a reference, an identical measurement was performed on the MWCNT/PDMS composite film, and the respective Raman spectra are shown in Figure 1d, which shows a similar trend in 2D peak shifts as hybrid nanocomposites. The compressive strains induced altering the geometric configurations of CNTs and xGnPs due to the interfacial adhesion between the carbon nanomaterials and PDMS. As the compressive load increases, the 2D peak of nanocomposites shows a blue shift, that is, a decrease in wavelength. The results demonstrate the spatial rearrangements of the carbon nanomaterials under compressive loading, and the interfacial adhesion is the underlying mechanisms that contribute to the piezoresistive behavior, which enables the hybrid nanocomposites to serve as compression sensors.

To evaluate the electromechanical properties of the xGnP/MWCNT/PDMS nanocomposites, two copper electrodes were attached to the top and bottom surfaces of the samples using a conductive epoxy bond to obtain accurate electric signals during the compression test (Figure 2a). An acrylic plate was fixed to the aluminum compression zig to prevent the sensor output from electric signal interferences (Figure 2b).

Table 1. Electromechanical Properties of the Hybrid Nanocomposites as a Function of the Size of xGnP, wt % of Fillers, and xGnP:MWCNT Ratio

filler type	total wt % of the filler	xGnP:MWCNT ratio	compressive modulus (MPa)	gauge factor
M5 and CM250	1	7:3	0.23	5.9
M5 and CM250	1	5:5	0.45	3.9
M5 and CM250	1	2:8	1.03	1.2
M5 and CM250	3	7:3	0.69	3.0
M5 and CM250	3	5:5	1.54	2.5
M5 and CM250	3	2:8	2.46	1.2
M15 and CM250	1	7:3	0.13	23.8
M15 and CM250	1	5:5	0.33	8.5
M15 and CM250	1	2:8	0.59	4.5
M15 and CM250	3	7:3	0.17	1.7
M15 and CM250	3	5:5	0.93	1.3
M15 and CM250	3	2:8	1.63	0.7
CM250	1	0:10	0.58	4.7
CM250	3	0:10	1.24	3.5

https://dx.doi.org/10.1021/acsomega.9b03012
ACS Omega 2020, 5, 2630−2639

Scheme 1. Fabrication Process of the Hybrid Nanocomposite

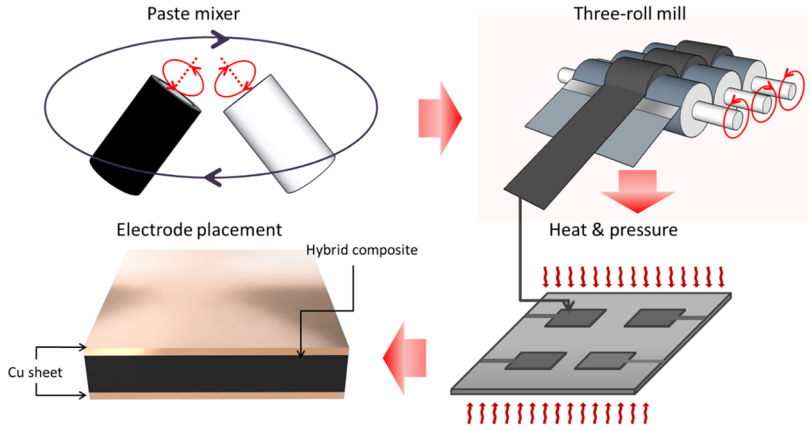

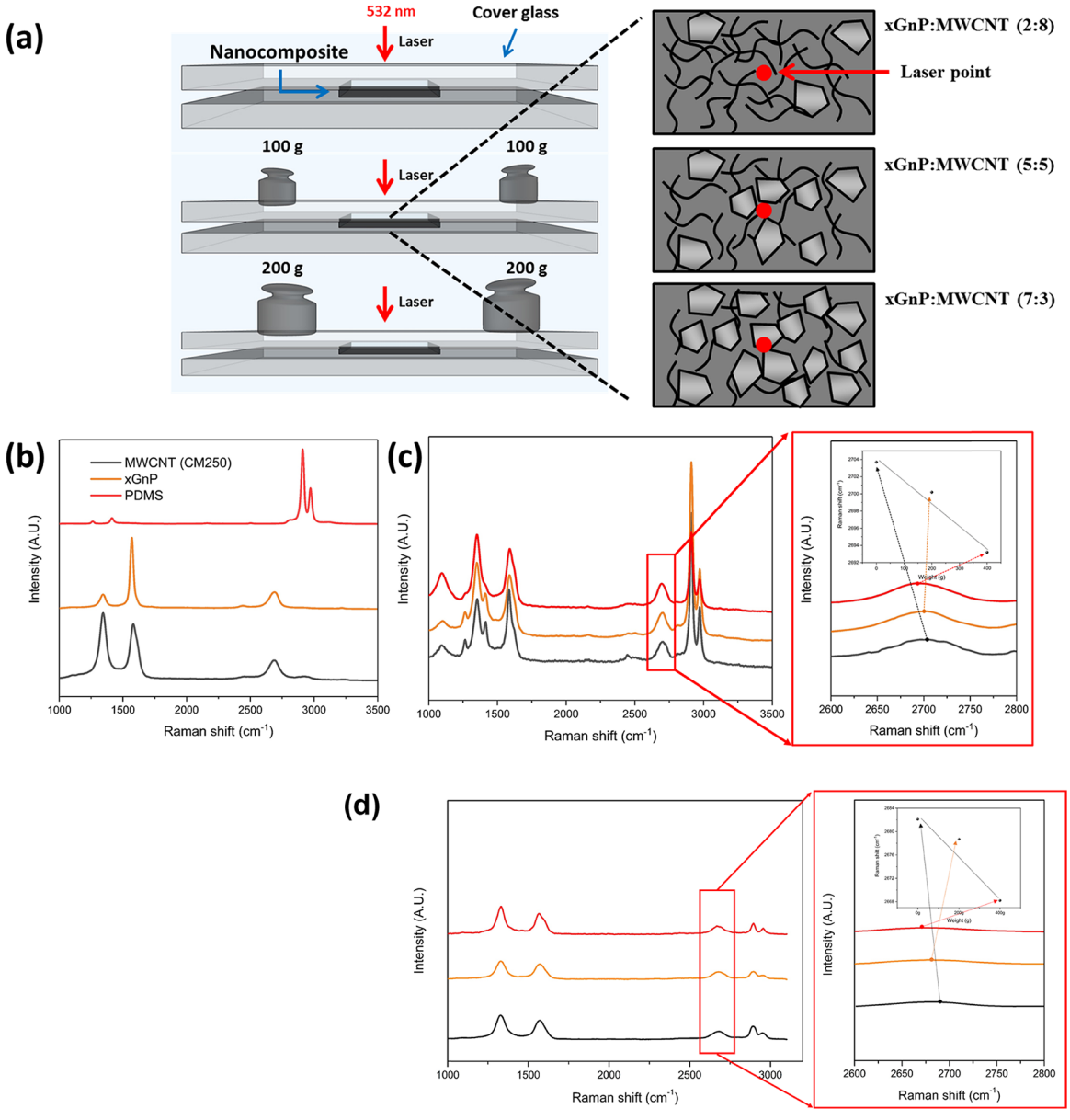

Figure 1. Raman analysis of the hybrid composites. (a) The schematic of the Raman analysis setup. (b) Raman spectra of pristine MWCNT (CM250), xGnP, and PDMS. (c) Raman spectra of xGnP:MWCNT (5:5) nanocomposite as the applied load increases. (d) Raman spectra of MWCNT/PDMS composite as the applied load increases. Magnified images in panels (c) and (d) show the 2D peaks (near 2700 cm^{-1}) in Raman spectra of nanocomposites showing the peak shift as the applied load increases.

https://dx.doi.org/10.1021/acsomega.9b03012
ACS Omega 2020, 5, 2630−2639

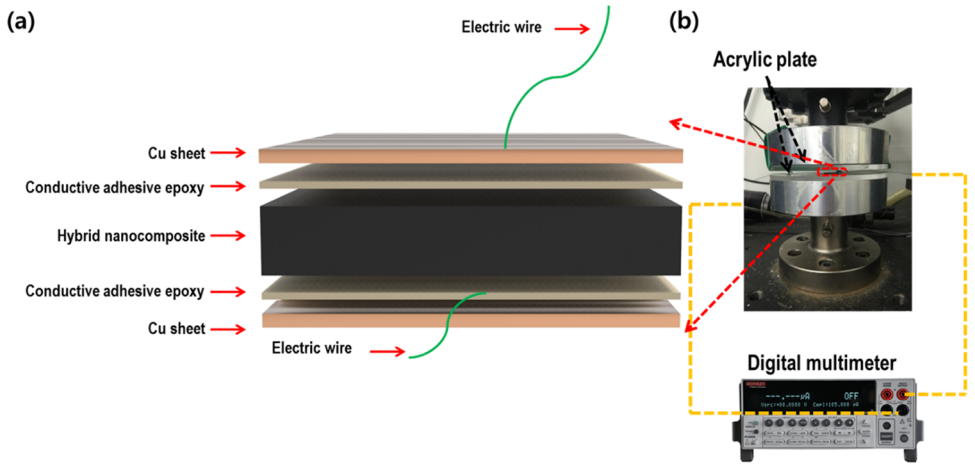

Figure 2. Sample configuration setup and piezoresistivity setup. (a) Sample configuration showing the electric signal transfer method under compression. (b) Piezoresistivity measurement setup. The inset photo shows compression jig, sample, and multimeter (Photograph courtesy of "Changyoon Jeong". Copyright 2019.).

To investigate the hybrid effect of the 1D MWCNTs and 2D xGnPs in hybrid nanocomposites, we used filler 1 and 3 wt %, various xGnP sizes, and xGnP:MWCNT ratios. Figure 3 shows

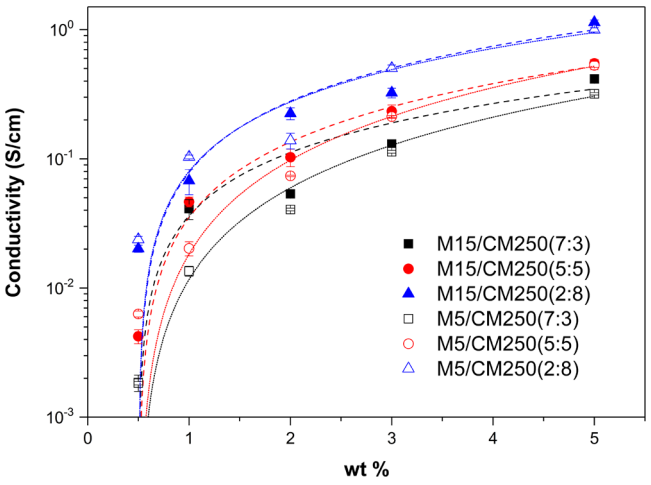

Figure 3. Electrical conductivity of the hybrid nanocomposites as a function of the xGnP:MWCNT ratio and wt % of nanofiller.

the conductivity of the hybrid nanocomposite consisting of the M15 xGnPs (large surface area (Figure 4a)) was higher than that of the composite consisting of the M5 xGnPs (small surface area (Figure 4b)) regardless of the xGnP:MWCNT ratio. The large surface area of M15 xGnP increases the number of contact points between MWCNTs and xGnPs, which facilitate the formation of conductive network under compression. In addition to the xGnP size effect, the conductivities of the xGnP M5 or M15/MWCNT/PDMS composites with various fillers ratios (7:3, 5:5, and 2:8) change with the composition of xGnP and MWCNT. An increase in the xGnP:MWCNT ratio resulted in a decrease in the conductivity of the hybrid composites, affecting compression sensing capabilities of the sensor due to a difference in initial resistance. In extremely low electrical conductivity, the electric responses of the sensor could hardly form conductive networks and were hampered by environmental (thermal or vibration) fluctuations. On the other hand, in very high electrical conductivity, the adverse effect of the contact resistance

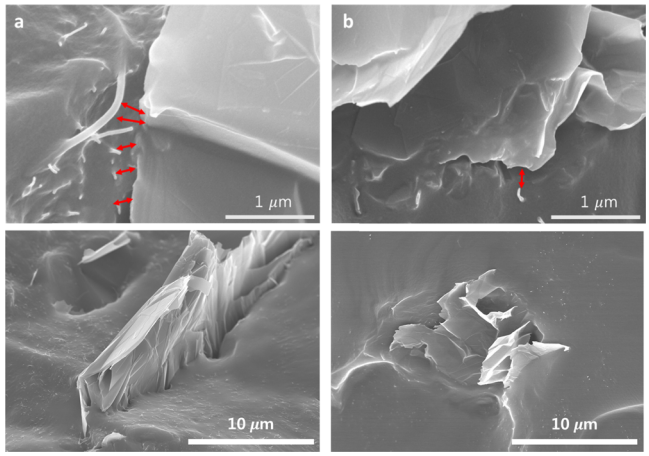

Figure 4. Cross-sectional SEM images of the hybrid composites: (a) M15 xGnP/CM250 and (b) M5 xGnP/CM250. Lower images are low-magnification images.

increases, and the sensitivity of the sensor decreases. Proper conductivity is very important in sensor design for sensing performance. The hybrid composite containing 1 wt % M15 xGnPs shows higher conductivity than that containing 1 wt % M5 xGnPs. This high conductivity facilitates the formation of new conductive networks under compression and influences sensitivity of the sensor. The 3 wt % hybrid nanocomposites, on the other hand, show too many conductive paths in the polymer matrix by lowering the sensitivity of the sensor. The generation of these conductive paths determines sensitivity of the sensor in response to compressive stress. This indicates that the proper conductivity of the composites affects the sensitivity of the sensor under compression. For the same reason, the effect of xGnP size is explained by the formation of conductive networks in the polymer matrix, affecting the sensitivity of the sensor. In addition to change of wt % and xGnP size, sensor sensitivity increases with an increase in their xGnP:MWCNT ratios. Nanocomposites with an xGnP:MWCNT ratio of 7:3 could readily form conductive networks under compression due to the strong interaction between the filler particles (Scheme 2). This bridge effects induced by the combination of the 1D and 2D nanofillers are observed in all kinds of samples under compression regardless

https://dx.doi.org/10.1021/acsomega.9b03012
ACS Omega 2020, 5, 2630−2639

Scheme 2. Compression-Sensing Mechanism of the Composites with Various xGnP:MWCNT Ratios (7:3, 5:5, and 2:8)

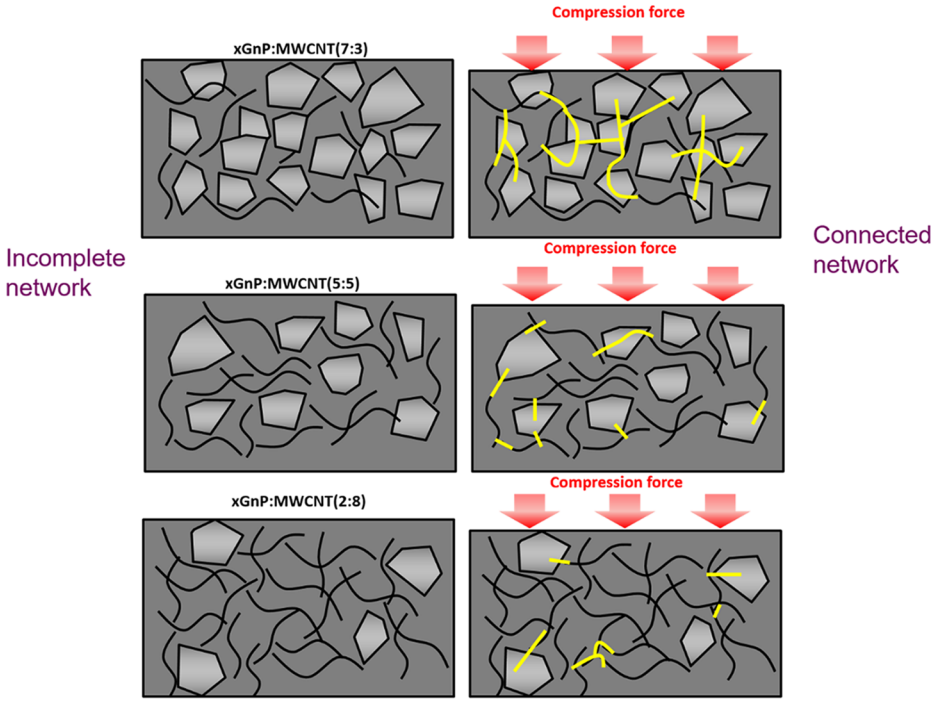

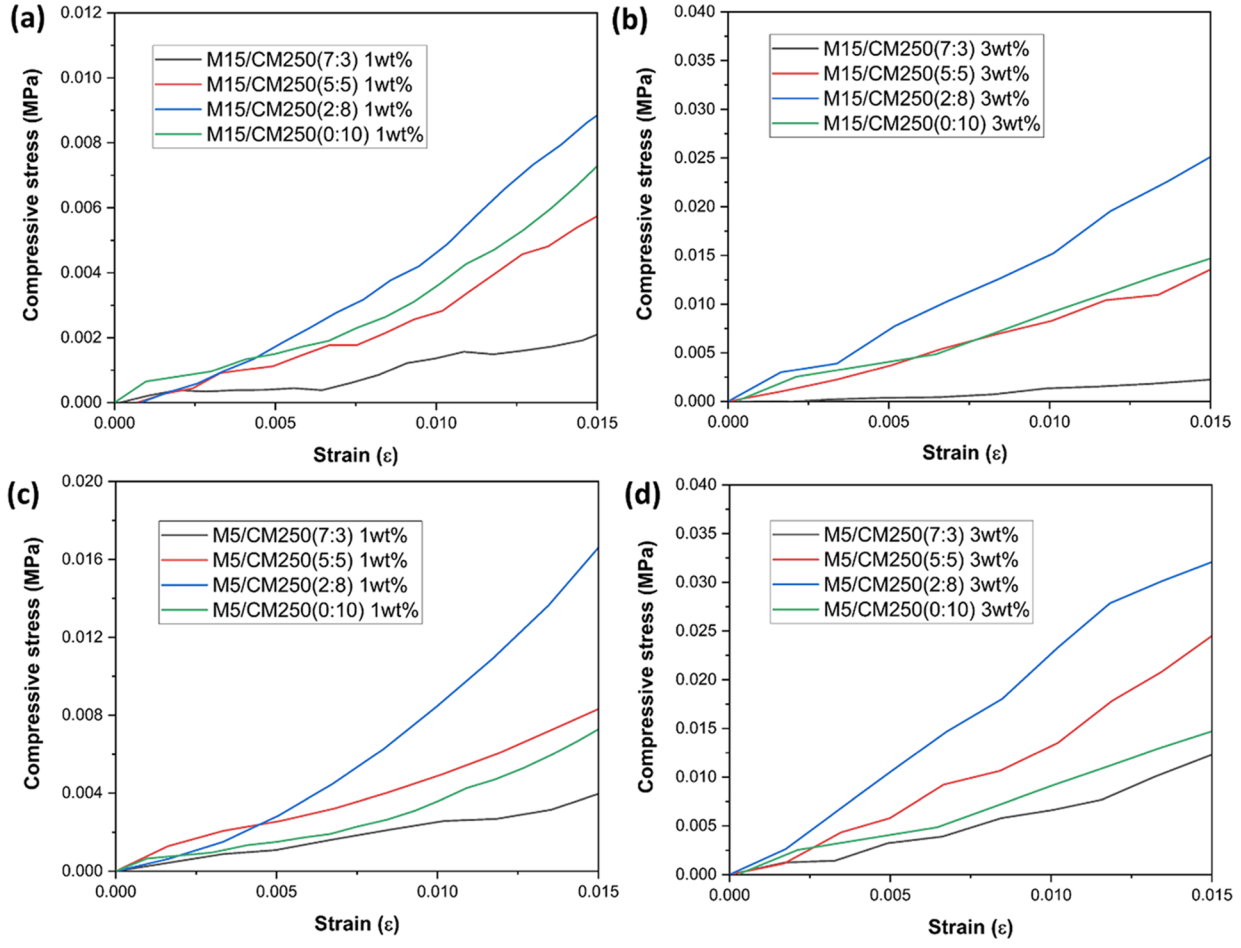

Figure 5. Compressive stress vs strain for (a) M15/CM250 7:3, 5:5, 2:8, and 0:10 (1 wt %), (b) M15/CM250 7:3, 5:5, 2:8, and 0:10 (3 wt %), (c) M5/CM250 7:3, 5:5, 2:8, and 0:10 (1 wt %), and (d) M5/CM250 7:3, 5:5, 2:8, and 0:10 (3 wt %).

https://dx.doi.org/10.1021/acsomega.9b03012
ACS Omega 2020, 5, 2630−2639

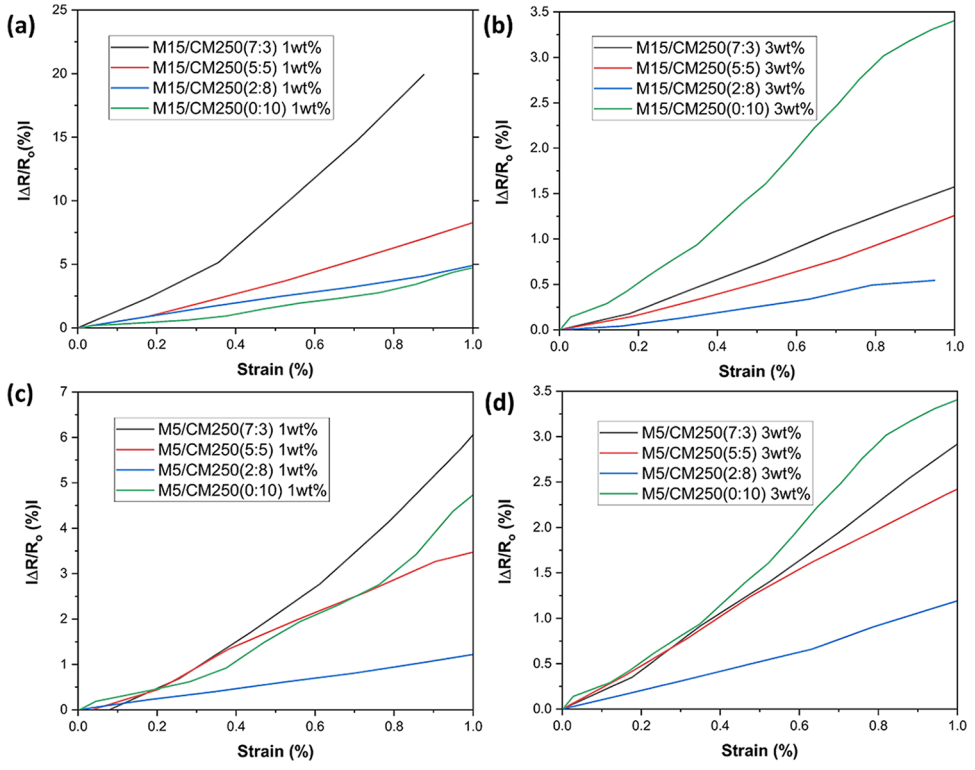

Figure 6. Normalized change in the electrical resistance vs compressive strain for (a) M15/CM250 7:3, 5:5, 2:8, and 0:10 (1 wt %), (b) M15/CM250 7:3, 5:5, 2:8, and 0:10 (3 wt %), (c) M5/CM250 7:3, 5:5, 2:8, and 0:10 (1 wt %), and (d) M5/CM250 7:3, 5:5, 2:8, and 0:10 (3 wt %).

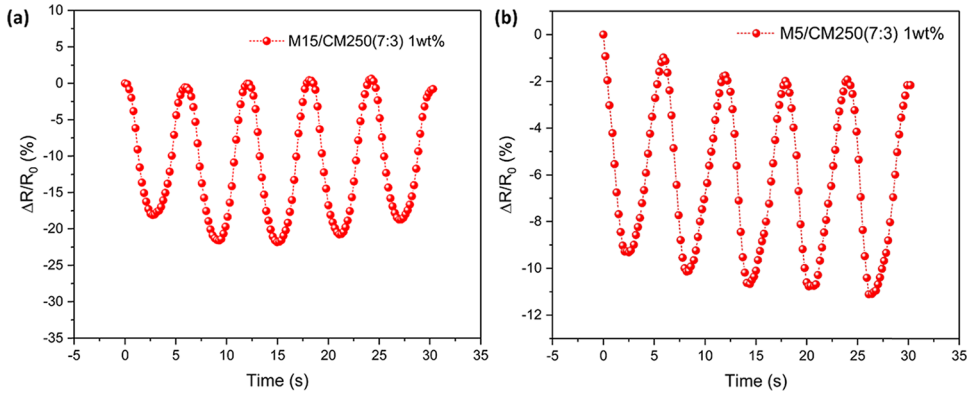

Figure 7. Cycling compressive loading of hybrid nanocomposites strained up to 1%. (a) Change of electrical resistance vs time for M15/CM250 7:3 (1 wt %) and (b) M5/CM250 7:3 (1 wt %).

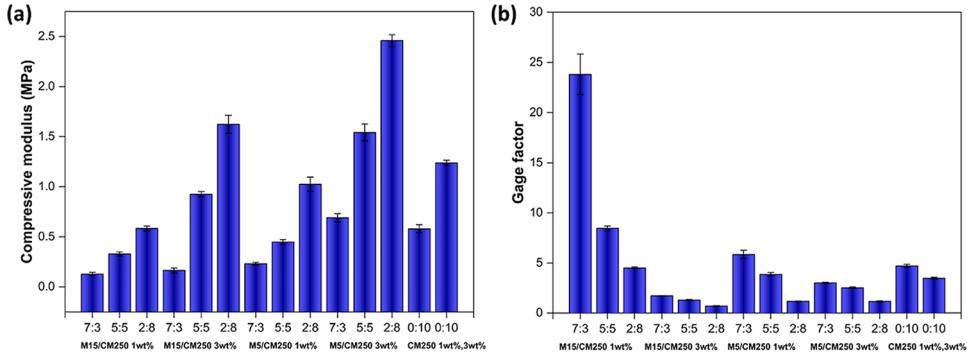

Figure 8. Compressive modulus (a) and gauge factors (b) of the hybrid nanocomposites with different xGnP sizes and weight fractions (1 and 3 wt %), xGnP:MWCNT ratios (7:3, 5:5, 2:8, and 0:10).

https://dx.doi.org/10.1021/acsomega.9b03012
ACS Omega 2020, 5, 2630−2639

of the xGnP size and wt % depending on the xGnP:MWCNT ratio. In terms of flexibility, Figure 5 shows that the rate of compressive stress increases with a decrease in the xGnP:MWCNT ratio regardless of the xGnP size and wt %. On the other hand, the sensitivity of the hybrid nanocomposites increases with an increase in the xGnP:MWCNT ratio (Figure 6). Thus, changes of flexibility and conductivity depending on the xGnP:MWCNT ratio determine the sensor sensitivity under compression. The amount of filler (wt %) significantly affects the mechanical and electrical properties of the hybrid nanocomposites. With an increase in the filler weight fraction from 1 to 3 wt % (Figure 5a–d), compressive stress of the composites increased when samples were subjected to the same compressive strain because the compressive load could be easily transferred from the polymer matrix to the filler. The sensitivity of nanocomposites increased with a decrease in the filler wt % because saturated conductive networks disturb the formation of additional conductive networks under compression (Figure 6a–d).

Figure 7 shows five compressive loading–unloading cycles exerted on hybrid nanocomposites, strained up to ∼1%. The relative resistance decreased with increasing compressive strains and was fully recovered upon releasing unloading in both M15 (Figure 7a) and M5 (Figure 7b) xGnP hybrid nanocomposites.

To better understand the effect of the amount of nanofiller on polymer, size of the nanofiller, and the ratio of the hybrid nanofiller, we compared compressive modulus depending on wt %, xGnP:MWCNT ratio, and xGnP size. Figure 8a shows that the compressive modulus increase is more obvious when wt % of filler in polymer increases. To illustrate the influence of xGnP size on mechanical properties, we used different sizes of xGnP, with 3 times the diameter difference, as the filler. Increasing compressive modulus can be observed with decreasing xGnP size in the nanocomposites containing hybrid fillers. The M5 xGnP could interact easily with the MWCNTs in the polymer matrix under compression as compared to the M15 xGnP in the same wt %. Regardless of xGnP size, we observed that, as the weight ratio of MWCNT in hybrid composites increases, the compressive modulus increases due to entanglement of MWCNT in fillers. Thus, the compressive modulus of the hybrid composites was determined by interaction between nanofillers.

For comparing sensitivity of the sensor under compression, the sensor sensitivity was quantified by the gauge factor defined as

$$\text{gauge factor} = \frac{\Delta R}{R_0} \cdot \frac{1}{\varepsilon} \quad (1)$$

where ΔR is the relative change in electrical resistance, R_0 is the initial electrical resistance, and ε is the compressive strain.

As shown in Figure 8b, wt %, xGnP:MWCNT ratio, and xGnP size influence the response to compressive strain. The gauge factor was mainly affected by the tunneling effect, which was strongly related to the distance between the nanofillers in the matrix under the compressive strain. The gauge factor of the sensor decreases with an increase in nanofiller weight fraction due to differences in flexibility. The flexibility of the nanocomposite depends on the CNT content in hybrid fillers, which also affects the sensitivity of the sensor. Increasing CNT content in the nanocomposites containing hybrid fillers weakens the sensitivity of the sensing in 1 and 3 wt % nanocomposites. Flexibility of the hybrid nanocomposite is also related to xGnP size. The hybrid composite with 1 wt % M15 xGnPs shows a higher gauge factor than the composite with 1 wt % M5 xGnPs under compression, showing the xGnP size effect. However, it can be seen that high conductivity due to high wt % affects the gauge factor. The results of changing CNTs and xGnP network structure, such as compressive modulus and gauge factor of nanocomposites, are summarized in Figure 9. As wt % of nanofillers increases, it reaches a point

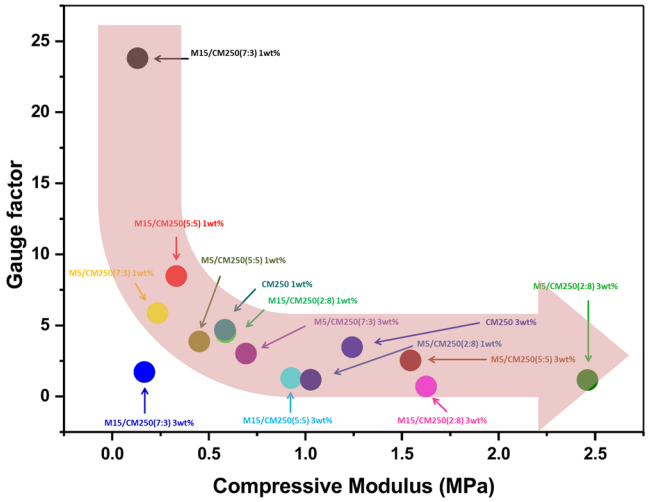

Figure 9. Gauge factor vs compressive modulus curves for various nanocomposites showing the relation between flexibility and gauge factor.

where additional conductive pathways do not significantly affect piezoresistivity under compression, while compressive modulus continues to increase. Figure 9 also illustrates the hybrid effect that it enables the formation of a conductive pathway via bridging the gaps between neighboring CNTs, which exhibit high gauge factors in hybrid nanocomposites compared to that in CNT composites. Therefore, flexibility and conductivity, which are influenced by wt %, hybrid filler ratio, and filler size, affect the electromechanical properties of the hybrid nanocomposites.

CONCLUSIONS

The electrical and mechanical properties of hybrid nanocomposites consisting of xGnPs, MWCNTs, and PDMS polymer under compression were investigated. An increase in the weight fraction of the nanofillers increased the compressive modulus and decreased the gauge factor of the composites. This indicates that the filler weight fraction affected the mechanical properties of the composites, while their compression sensitivity was affected by the formation of additional conductive networks during compression. The xGnP size affects the electrical and mechanical properties of the hybrid nanocomposites. The nanocomposite with the M5 xGnPs shows better mechanical properties than that with the M15 xGnPs. However, the electrical properties of the composites depend on both the size and wt % of the nanofiller. In addition to these factors, the mechanical and electrical properties of hybrid nanocomposites were strongly related to the xGnP:MWCNT ratio regardless of the size and wt % of the nanofiller. The compressive modulus of the nanocomposites increases with a decrease in the

https://dx.doi.org/10.1021/acsomega.9b03012
ACS Omega 2020, 5, 2630–2639

xGnP:MWCNT ratio. This is because the dense 1D fillers strongly interlocked the 2D fillers and the polymer in low xGnP:MWCNT ratios. With an increase in the xGnP:MWCNT ratio, the gauge factor of nanocomposites increases because the "preplaced" 2D conductive fillers easily interacted with the 1D conductive fillers under compression. Hence, it can be stated that the xGnP size, xGnP:MWCNT ratio, and nanofiller wt % affect the compressive modulus and sensitivity of the nanocomposites under compression.

EXPERIMENTAL SECTION

Materials. The xGnPs (M5 and M15) used in this study were provided by XG Sciences. These xGnPs showed excellent electrical conductivity (parallel to surface: 10^7 S/m, perpendicular to surface: 10^2 S/m), a thickness of 6−8 nm, and average particle diameters of 5 (M5) and 15 μm (M15). The MWCNTs (CM250) used in this study were provided by Hanwha Chemical (Incheon, Korea). These MWCNTs had a length of 60−70 μm and a diameter of 3.5−4 nm. The MWCNTs showed a high aspect ratio (2×10^4), electrical conductivity (10^7 S/m), and dispersibility, which are important properties for sensor filler materials. The PDMS silicon-based organic polymer used as the matrix was purchased from SaeHwang Hi-tech. It showed a very low glass transition temperature (−125 °C), low shrinkage rate, ease of fabrication, and elastomer characteristics. The flexibility and sensitivity of the sensor fabricated in this study, which could be easily deformed by compressive strain, depended on the properties of the PDMS matrix.

Characterization. The morphologies of the hybrid nanofillers were characterized using field-emission scanning electron microscopy (FE-SEM; S-4800, Hitachi). Raman spectra were measured by scattered radiation of different wavelengths (confocal Raman; alpha300R, WITec). For measurement of compression behavior of the sample, cover glass and weight enable us to measure Raman spectra at pressures down to several compression forces. The electrical conductivity of nanocomposites was measured by a four-point probe (CMT-SR1000N). The compression tests were carried out on a universal material testing system (Instron 5982) at a compressive strain speed of 1 mm/min at ambient temperature. The electrical signals were captured using a Keithley 2002 multimeter and a 7001-switching system, which were operated by programmed data acquisition software for compression.

AUTHOR INFORMATION

Corresponding Author

Young-Bin Park − *Department of Mechanical Engineering, Ulsan National Institute of Science and Technology, Ulsan 44919, Republic of Korea;* orcid.org/0000-0001-5936-7155; Email: ypark@unist.ac.kr

Author

Changyoon Jeong − *Department of Mechanical Engineering, Ulsan National Institute of Science and Technology, Ulsan 44919, Republic of Korea*

Complete contact information is available at: https://pubs.acs.org/10.1021/acsomega.9b03012

Notes

The authors declare no competing financial interest.

ACKNOWLEDGMENTS

This research was financially supported by the Nano-Material Technology Development Program through the National Research Foundation (NRF) funded by the Ministry of Science and ICT of Korea (Grant No. 2016M3A7B4027697) and the 2019 Research Fund (1.190009) of UNIST (Ulsan National Institute of Science and Technology).

REFERENCES

(1) Kumar, S.; Bisoyi, H. K. Aligned Carbon Nanotubes in the Supramolecular Order of Discotic Liquid Crystals. *Angew. Chem.* **2007**, *119*, 1523−1525.

(2) Bouhamed, A.; Al-Hamry, A.; Müller, C.; Choura, S.; Kanoun, O. Assessing the electrical behaviour of MWCNTs/epoxy nanocomposite for strain sensing. *Composites, Part B* **2017**, *128*, 91−99.

(3) Zhou, H. W.; Mishnaevsky, L., Jr.; Yi, H. Y.; Liu, Y. Q.; Hu, X.; Warrier, A.; Dai, G. M. Carbon fiber/carbon nanotube reinforced hierarchical composites: Effect of CNT distribution on shearing strength. *Composites, Part B* **2016**, *88*, 201−211.

(4) Tan, D.; Zhao, J.; Gao, C.; Wang, H.; Chen, G.; Shi, D. Carbon Nanoparticle Hybrid Aerogels: 3D Double-Interconnected Network Porous Microstructure, Thermoelectric, and Solvent-Removal Functions. *ACS Appl. Mater. Interfaces* **2017**, *9*, 21820−21828.

(5) Wang, Q.; Dai, J.; Li, W.; Wei, Z.; Jiang, J. The effects of CNT alignment on electrical conductivity and mechanical properties of SWNT/epoxy nanocomposites. *Compos. Sci. Technol.* **2008**, *68*, 1644−1648.

(6) Sasmal, S.; Ravivarman, N.; Sindu, B. S.; Vignesh, K. Electrical conductivity and piezo-resistive characteristics of CNT and CNF incorporated cementitious nanocomposites under static and dynamic loading. *Composites, Part A* **2017**, *100*, 227−243.

(7) Xu, H.; Zeng, Z.; Wu, Z.; Zhou, L.; Su, Z.; Liao, Y.; Liu, M. Broadband dynamic responses of flexible carbon black/poly (vinylidene fluoride) nanocomposites: A sensitivity study. *Compos. Sci. Technol.* **2017**, *149*, 246−253.

(8) Zhao, J.; Dai, K.; Liu, C.; Zheng, G.; Wang, B.; Liu, C.; Chen, J.; Shen, C. A comparison between strain sensing behaviors of carbon black/polypropylene and carbon nanotubes/polypropylene electrically conductive composites. *Composites, Part A* **2013**, *48*, 129−136.

(9) Han, B.; Zhang, L.; Sun, S.; Yu, X.; Dong, X.; Wu, T.; Ou, J. Electrostatic self-assembled carbon nanotube/nano carbon black composite fillers reinforced cement-based materials with multifunctionality. *Composites, Part A* **2015**, *79*, 103−115.

(10) Luheng, W.; Tianhuai, D.; Peng, W. Influence of carbon black concentration on piezoresistivity for carbon-black-filled silicone rubber composite. *Carbon* **2009**, *47*, 3151−3157.

(11) Kim, T.; Park, J.; Sohn, J.; Cho, D.; Jeon, S. Bioinspired, Highly Stretchable, and Conductive Dry Adhesives Based on 1D-2D Hybrid Carbon Nanocomposites for All-in-One ECG Electrodes. *ACS Nano* **2016**, *10*, 4770−4778.

(12) Romano, M. S.; Li, N.; Antiohos, D.; Razal, J. M.; Nattestad, A.; Beirne, S.; Fang, S.; Chen, Y.; Jalili, R.; Wallace, G. G.; Baughman, R.; Chen, J. Carbon nanotube - reduced graphene oxide composites for thermal energy harvesting applications. *Adv. Mater.* **2013**, *25*, 6602−6606.

(13) Li, J.; Lai, C.; Jia, X.; Wang, L.; Xiang, X.; Ho, C.-L.; Li, H.; Wong, W.-Y. Effect of electron donor/acceptor substituents on the Seebeck coefficient and thermoelectric properties of poly(3-methylthiophene methine)s/graphite composites. *Composites, Part B* **2015**, *77*, 248−256.

(14) Cheng, Q.; Tang, J.; Ma, J.; Zhang, H.; Shinya, N.; Qin, L. C. Graphene and carbon nanotube composite electrodes for supercapacitors with ultra-high energy density. *Phys. Chem. Chem. Phys.* **2011**, *13*, 17615−17624.

(15) Stankovich, S.; Dikin, D. A.; Dommett, G. H. B.; Kohlhaas, K. M.; Zimney, E. J.; Stach, E. A.; Piner, R. D.; Nguyen, S. T.; Ruoff, R. S. Graphene-based composite materials. *Nature* **2006**, *442*, 282−286.

https://dx.doi.org/10.1021/acsomega.9b03012
ACS Omega 2020, 5, 2630−2639

(16) Liu, C.; Yang, S. Synthesis of Angstrom-Scale Anatase Titania Atomic Wires. *ACS Nano* **2009**, *3*, 1025−1031.
(17) Fierke, C. A.; Hammes, G. G. Transient kinetic approaches to enzyme mechanisms. In *Contemporary Enzyme Kinetics and Mechanism*; 2nd ed.; Purich, D., Ed.; Academic Press: Cambridge, MA, 1996, 1−35.
(18) Moreau, P.; Anizon, F.; Sancelme, M.; Prudhomme, M.; Bailly, C.; Sevère, D.; Riou, J. F.; Fabbro, D.; Meyer, T.; Aubertin, A. M. Syntheses and Biological Activities of Rebeccamycin Analogues. Introduction of a Halogenoacetyl Substituent. *J. Med. Chem.* **1999**, *42*, 584−592.
(19) Kwon, D.-J.; Wang, Z.-J.; Choi, J.-Y.; Shin, P.-S.; DeVries, K. L.; Park, J.-M. Damage sensing and fracture detection of CNT paste using electrical resistance measurements. *Composites, Part B* **2016**, *90*, 386−391.
(20) Bilotti, E.; Zhang, R.; Deng, H.; Baxendale, M.; Peijs, T. Fabrication and property prediction of conductive and strain sensing TPU/CNT nanocomposite fibres. *J. Mater. Chem.* **2010**, *20*, 9449.
(21) Ma, P.-C.; Siddiqui, N. A.; Marom, G.; Kim, J.-K. Dispersion and functionalization of carbon nanotubes for polymer-based nanocomposites: A review. *Composites, Part A* **2010**, *41*, 1345−1367.
(22) Liebscher, M.; Gärtner, T.; Tzounis, L.; Mičušík, M.; Pötschke, P.; Stamm, M.; Heinrich, G.; Voit, B. Influence of the MWCNT surface functionalization on the thermoelectric properties of melt-mixed polycarbonate composites. *Compos. Sci. Technol.* **2014**, *101*, 133−138.
(23) Wang, L.; Jiang, F.; Xiong, J.; Xu, J.; Zhou, W.; Liu, C.; Shi, H.; Jiang, Q. Effects of second dopants on electrical conductivity and thermopower of poly(3,4-ethylenedioxythiophene):poly-(styrenesulfonate)-filled carbon black. *Mater. Chem. Phys.* **2015**, *153*, 285−290.
(24) Švorčík, V.; Miček, I.; Jankovskij, O.; Rybka, V.; Hnatowicz, V.; Wang, L.; Angert, N. Electrical resistivity and thermoelectric power of carbon black loaded polyethylene modified by GeV ion irradiation. *Polym. Degrad. Stab.* **1997**, *55*, 115.
(25) Yan, C.; Wang, J.; Kang, W.; Cui, M.; Wang, X.; Foo, C. Y.; Chee, K. J.; Lee, P. S. Highly stretchable piezoresistive graphene-nanocellulose nanopaper for strain sensors. *Adv. Mater.* **2014**, *26*, 2022−2027.
(26) Boland, C. S.; Khan, U.; Backes, C.; O'Neill, A.; McCauley, J.; Duane, S.; Shanker, R.; Liu, Y.; Jurewicz, I.; Dalton, A. B.; Coleman, J. N. Sensitive, high-strain, high-rate bodily motion sensors based on graphene-rubber composites. *ACS Nano* **2014**, *8*, 8819−8830.
(27) Littlejohn, S.; Nogaret, A.; Prentice, G. M.; Pantos, G. D. Pressure Sensing and Electronic Amplification with Functionalized Graphite-Silicone Composite. *Adv. Funct. Mater.* **2013**, *23*, 5398−5402.
(28) Kumar, R.; Singh, R.; Hui, D.; Feo, L.; Fraternali, F. Graphene as biomedical sensing element: State of art review and potential engineering applications. *Composites, Part B* **2018**, *134*, 193−206.
(29) Wang, X.; Meng, S.; Tebyetekerwa, M.; Li, Y.; Pionteck, J.; Sun, B.; Qin, Z.; Zhu, M. Highly sensitive and stretchable piezoresistive strain sensor based on conductive poly(styrene-butadiene-styrene)/few layer graphene composite fiber. *Composites, Part A* **2018**, *105*, 291−299.
(30) Balaji, R.; Sasikumar, M. Graphene based strain and damage prediction system for polymer composites. *Composites, Part A* **2017**, *103*, 48−59.
(31) Xia, X.; Chen, J.; Liu, G.; Javed, M. S.; Wang, X.; Hu, C. Aligning graphene sheets in PDMS for improving output performance of triboelectric nanogenerator. *Carbon* **2017**, *111*, 569−576.
(32) Chen, H.; Xu, Y.; Bai, L.; Jiang, Y.; Zhang, J.; Zhao, C.; Li, T.; Yu, H.; Song, G.; Zhang, N.; Gan, Q. Crumpled Graphene Triboelectric Nanogenerators: Smaller Devices with Higher Output Performance. *Adv. Mater. Technol.* **2017**, *2*, 1700044.
(33) Kumar, A.; Ghosh, P. K.; Yadav, K. L.; Kumar, K. Thermo-mechanical and anti-corrosive properties of MWCNT/epoxy nano-composite fabricated by innovative dispersion technique. *Composites, Part B* **2017**, *113*, 291−299.
(34) Ferreira, A.; Cardoso, P.; Klosterman, D.; Covas, J. A.; van Hattum, F. W. J.; Vaz, F.; Lanceros-Mendez, S. Effect of filler dispersion on the electromechanical response of epoxy/vapor-grown carbon nanofiber composites. *Smart Mater. Struct.* **2012**, *21*, No. 075008.
(35) Hong, J. S.; Kim, C. Dispersion of multi-walled carbon nanotubes in PDMS/PB blend. *Rheol. Acta* **2011**, *50*, 955−964.
(36) Li, J.; Ma, P. C.; Chow, W. S.; To, C. K.; Tang, B. Z.; Kim, J. K. Correlations between Percolation Threshold, Dispersion State, and Aspect Ratio of Carbon Nanotubes. *Adv. Funct. Mater.* **2007**, *17*, 3207−3215.
(37) Kashiwagi, T.; Fagan, J.; Douglas, J. F.; Yamamoto, K.; Heckert, A. N.; Leigh, S. D.; Obrzut, J.; Du, F.; Lin-Gibson, S.; Mu, M.; Winey, K. I.; Haggenmueller, R. Relationship between dispersion metric and properties of PMMA/SWNT nanocomposites. *Polymer* **2007**, *48*, 4855−4866.
(38) Park, J.; Lee, Y.; Hong, J.; Ha, M.; Jung, Y.-D.; Lim, H.; Kim, S. Y.; Ko, H. Giant tunneling piezoresistance of composite elastomers with interlocked microdome arrays for ultrasensitive and multimodal electronic skins. *ACS Nano* **2014**, *8*, 4689−4697.
(39) Bao, W. S.; Meguid, S. A.; Zhu, Z. H.; Weng, G. J. Tunneling resistance and its effect on the electrical conductivity of carbon nanotube nanocomposites. *J. Appl. Phys.* **2012**, *111*, No. 093726.
(40) Hu, N.; Karube, Y.; Yan, C.; Masuda, Z.; Fukunaga, H. Tunneling effect in a polymer/carbon nanotube nanocomposite strain sensor. *Acta Mater.* **2008**, *56*, 2929−2936.
(41) Avilés, F.; May-Pat, A.; López-Manchado, M. A.; Verdejo, R.; Bachmatiuk, A.; Rümmeli, M. H. A comparative study on the mechanical, electrical and piezoresistive properties of polymer composites using carbon nanostructures of different topology. *Eur. Polym. J.* **2018**, *99*, 394−402.
(42) Guo, A.; Roso, M.; Modesti, M.; Liu, J.; Colombo, P. Preceramic polymer-derived SiOC fibers by electrospinning. *J. Appl. Polym. Sci.* **2014**, *131*, 39836.
(43) An, Y.; Tai, Z.; Qi, Y.; Yan, X.; Liu, B.; Xue, Q.; Pei, J. Friction and wear properties of graphene oxide/ultrahigh-molecular-weight polyethylene composites under the lubrication of deionized water and normal saline solution. *J. Appl. Polym. Sci.* **2014**, *131*, 39640.
(44) Aguilar-Bolados, H.; Yazdani-Pedram, M.; Contreras-Cid, A.; López-Manchado, M. A.; May-Pat, A.; Avilés, F. Influence of the morphology of carbon nanostructures on the piezoresistivity of hybrid natural rubber nanocomposites. *Composites, Part B* **2017**, *109*, 147−154.
(45) Zhao, H.; Bai, J. Highly sensitive piezo-resistive graphite nanoplatelet-carbon nanotube hybrids/polydimethylsilicone composites with improved conductive network construction. *ACS Appl. Mater. Interfaces* **2015**, *7*, 9652−9659.
(46) Zheng, Y.; Li, Y.; Dai, K.; Wang, Y.; Zheng, G.; Liu, C.; Shen, C. A highly stretchable and stable strain sensor based on hybrid carbon nanofillers/polydimethylsiloxane conductive composites for large human motions monitoring. *Composites Science and Technology* **2018**, *156*, 276−286.
(47) Natarajan, T. S.; Eshwaran, S. B.; Stöckelhuber, K. W.; Wießner, S.; Pötschke, P.; Heinrich, G.; Das, A. Strong Strain Sensing Performance of Natural Rubber Nanocomposites. *ACS Appl. Mater. Interfaces* **2017**, *9*, 4860−4872.
(48) Ma, P. C.; Liu, M. Y.; Zhang, H.; Wang, S. Q.; Wang, R.; Wang, K.; Wong, Y. K.; Tang, B. Z.; Hong, S. H.; Paik, K. W.; Kim, J. K. Enhanced electrical conductivity of nanocomposites containing hybrid fillers of carbon nanotubes and carbon black. *ACS Appl. Mater. Interfaces* **2009**, *1*, 1090−1096.
(49) Huang, Y.; Wang, W.; Wang, Y.; Liu, P.; Liu, C.; Tian, H. Synergistic effects and piezoresistive characteristics of carbon nanofillers/silicone rubber composites. *Mater. Technol.* **2015**, *31*, 229.
(50) Schadler, L. S.; Giannaris, S. C.; Ajayan, P. M. Load transfer in carbon nanotube epoxy composites. *Appl. Phys. Lett.* **1998**, *73*, 3842−3844.

https://dx.doi.org/10.1021/acsomega.9b03012
ACS Omega 2020, 5, 2630−2639

(51) Frank, O.; Tsoukleri, G.; Parthenios, J.; Papagelis, K.; Riaz, I.; Jalil, R.; Novoselov, K. S.; Galiotis, C. Compression Behavior of Single-Layer Graphenes. *ACS Nano* **2010**, *4*, 3131−3138.

https://dx.doi.org/10.1021/acsomega.9b03012
ACS Omega 2020, 5, 2630−2639